RSC Advances

ROYAL SOCIETY OF CHEMISTRY

www.rsc.org/advances

Journal Name

ARTICLE

Preparation of Colloidal Photonic Crystal containing CuO Nanoparticles with Tunable Structural Colors

Received 00th January 20xx,
Accepted 00th January 20xx

DOI: 10.1039/x0xx00000x

www.rsc.org/

Chun-Feng Lai,*[a] Yu-Chi Wang,[a] Chia-Lung Wu,[b] Jia-Yu Zeng,[a] and Chia-Feng Lin[b]

Polystyrene (PS) colloidal photonic crystal (CPhC) structures containing copper oxide nanoparticles (CuO NPs) present tunable structural colors, which are highly useful properties. We prepared PS CPhC color films containing CuO NPs using self-assembly of gravitational sedimentation method by electrostatic interactions. Incorporating CuO NPs into PS CPhC color films dramatically changed structural color without affecting the structure quality of CPhCs. The iridescent structural color of CuO–PS CPhC films was based on Bragg diffraction and backward scattering absorption using CuO NPs. The structural color of CuO–PS CPhC films was measured using color measurements under the Commission International d'Eclairage standard colorimetric system. The random adsorption of CuO NPs on PS nanospheres affected the photonic stop band, resulting in structural color changes. This study presents a simple and inexpensive method to produce tunable structural color for numerous applications, such as in decorative, security, textile fabrics, bionic colors, and optical devices.

Introduction

Structural colors generated by nanostructures are divided into iridescent color[1–4] and non-iridescent color[5–7]. Iridescent colors produced by the interaction of light with periodic structures have been of considerable interest[8-10]. The structure can be artificially fabricated by Bragg interference of multiple lights reflected inside periodic lattice crystals, such as colloidal photonic crystals (CPhCs)[11-13]. CPhC nanostructures have attracted great interest for providing new approaches to control photons. The self-assembly of polystyrene (PS) nanospheres into a close-packed array is a simple method of fabricating 3D CPhC structural color films. PS nanospheres assembled into periodic structures can produce structural color because of the interaction with visible light through interference, diffraction, and scattering[14,15]. However, several problems with CPhC structures include poor crystal quality because of cracks, which limit functional structural color for applications.

The structural color of CPhCs is extremely dull because of the interferences of scattering and background light. Therefore, several groups have reported the use of carbon (CB)[16-20] and metal nanoparticles (NPs)[21-27] materials to enhance the structural color of CPhCs. For example, Aguirre (2010) prepared colloidal pigments by mixing poly(methyl methacrylate) CPhCs with CB NPs[17]. Yamada (2010) fabricated CPhCs from nanoporous CB nanospheres and clearly enhanced brilliant structural colors[18]. Cong (2013) prepared CB NPs infiltrated into the voids of PS CPhCs to improve structural colors[19]. Pakkanen (2015) reported gold (Au) and silver (Ag) NPs infiltrated CPhCs to enhance localized surface plasmon resonance and structural color[27]. Table S1 overviewed methods to enhance the structural color of CPhCs. CPhC structures incorporating CB NPs exhibited easy to enhance the brilliant iridescent colors because CB NPs can absorb and scatter light. In addition, CPhC structures containing Au or Ag NPs demonstrated the localized surface plasmon resonance (LSPR) properties. CPhC structures containing CB, Au, or Ag NPs have been widely discussed in the previous literature. However, CPhCs incorporated with Copper (Cu) NPs have not yet been investigated. Cu nanopowders have general to use in biomedical applications as an antimicrobial[28] and a catalyst[29]. Therefore, we expected CPhCs incorporated with Cu NPs which could some advantages such as tunable photonic stop band (PSB), and Cu NPs is inexpensive than CB, Au, and Ag NPs.

CPhC structures allow the transmission of certain wavelengths and the reflection of other wavelengths. However, certain unavoidable defects in CPhCs decrease the reflectivity of the PSB and scatter the light outside the band, resulting in an opalescent appearance. Cu metal is prone surface oxidation on atmospheric environment at room temperature[30]. In this study, the dopant copper oxide (CuO) NPs in the CPhC structures could absorb all wavelengths and scatter light, thereby remarkably enhancing color and producing iridescent, tunable structural colors that were visible under natural lighting conditions. Thus, we added a small amount of CuO NPs to the colloidal PS latex. The main method for random adsorbing CuO NPs on PS nanospheres involved electrostatic interactions. In addition, the doping of CuO NPs into PS

[a] Department of Photonics, Feng Chia University, No. 100, Wenhwa Road, Seatwen, Taichung 40724, Taiwan. *E-mail: chunflai@fcu.edu.tw
[b] Department of Materials Science and Engineering, National Chung Hsing University, Taichung 402, Taiwan

†Electronic Supplementary Information (ESI) available: Structural parameters for three PS CPhC films used in this study. Transmittance and extinction spectra of CuO NPs solutions. Photographs of PS CPhC films prepared without and with CuO NPs. Reflection spectra of PS CPhC films without and with CuO NPs. See DOI: 10.1039/x0xx00000x

nanospheres and sedimentation on the bottom of substrate could absorb background and scattering light because CuO (ρ_{CuO} = 6.315 g cm^{-3}) has larger density than PS (ρ_{PS} = 0.96 g cm^{-3}), resulting in vivid structural colors. The reflection wavelengths of PS CPhC films with and without the CuO NPs were predicted theoretically and compared with experimental results. The structural color of the CuO–PS CPhC films was not only substantially enhanced but also varied with observation angles throughout the composition.

Experimental section

Materials

Styrene (St; Acros Organics) was distilled prior to use. Sodium dodecyl sulfate (SDS; Acros Organics), potassium persulphate (KPS; Acros Organics), sodiumbicarbonate ($NaHCO_3$; SHOWA), sulfuric acid (H_2SO_4; Aencore), hydrogen peroxide (H_2O_2; SHOWA), and Cu nanopowder (40—60 nm NP size; ≥99.5% trace metals basis; Sigma–Aldrich), were used as received. Deionized (DI) water was purified using PURELAB purification system. Cover glasses (Marienfeld) were immersed in a mixture of H_2SO_4 and H_2O_2 (volumetric ratio 7:3) for 2 h and then washed with DI water for several times to obtain a hydrophilic surface.

Synthesis of monodisperse polystyrene nanospheres

Negatively charged PS nanospheres were synthesized as follows[27]. The monodisperse PS nanospheres were prepared using St as monomer, SDS as emulsifier, KPS as initiator, and $NaHCO_3$ as buffer in the emulsion polymerization process[31,32]. SDS was used to provide the surface of PS nanospheres with a negative charge[27]. In the synthesis of sample B, 150 mg of SDS, 125 mg of $NaHCO_3$, and 200 mL of DI water were added to a 500 mL three-necked flask, which was placed in a water bath at 70 °C under nitrogen protection while stirring at 300 rpm. After 10 min, 15 mL of styrene and 250 mg of KPS dissolved in 50 mL of DI water were added to the mixture. After stirring for 24 h, monodisperse PS nanospheres with an average diameter (D_{PS}) of 230 nm were obtained. PS nanosphere powders were purified by dialysis, collected through centrifugation at 15,000 rpm for 1 h, and purified for three times through DI water washing before being dried in a vacuum drying oven. By varying the quantity of SDS, colloidal PS nanospheres with different sizes were synthesized using the same method, and the diameter of PS nanospheres was found to be linearly dependent on the amount of SDS (Fig. 1 and Tab. S2).

Preparation of colloidal PS suspensions incorporated with CuO NPs

Cu nanopowder was purchased from Sigma–Aldrich. Because Cu NPs are easily oxidized upon exposure to ambient laboratory atmosphere at room temperature, we utilized the random adsorption of CuO NPs on negatively charged PS nanospheres. PS latex suspensions containing 500 mg of three different diameters of PS nanosphere powder (samples A–C, Tab. S1) dispersed in 10 g of DI water at a concentration of approximately 4.8 weight percent (wt.%) were prepared by ultrasonication for 8 h. Various 4.8 wt.% PS latex suspensions were added with 0.05, 0.10, and 0.50 wt.% Cu nanopowder content. CuO NPs random distribution on PS by electrostatic interactions was allowed to occur with ultrasonication for 8 h, leading to unabsorbed CuO NPs settling on the bottom of the bottle (Fig. S2).

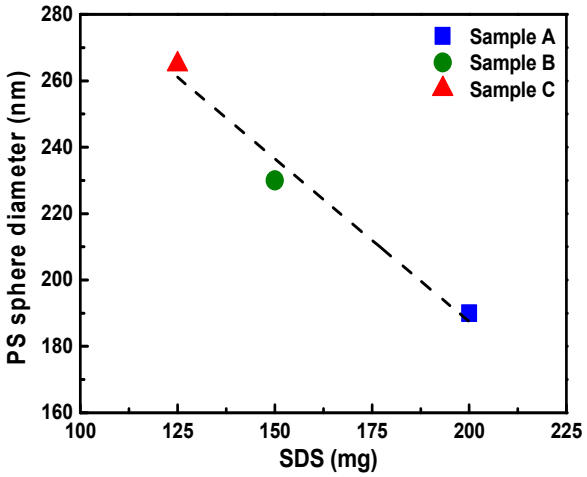

Figure 1. Diameter of colloidal PS nanospheres was dependent on the amount of SDS. The black dashed line indicates linear fitting.

Characterization

The morphologies of CuO–PS CPhC films were observed using field-emission scanning electron microscopy (FESEM; S–4800, Hitachi). Energy dispersive spectrometer (EDS; EMAX400, Horiba) was used to verify the presence of CuO NPs in PS CPhC films. The UV-Visible extinction measurements in a standard transmittance mode, and the reflectance, and the color measurement of CuO–PS CPhC films, were measured using a HR2000 spectrometer (Ocean Optics) with unpolarized white light provided by a Xe light source. The angle–resolved specular reflection setup contained a collected light from a CP140 spectrophotometer with a Sygnature charge-coupled device (CCD) detector (Jobin Yvon, Horiba). A fiber-coupled Xe lamp was used as a white light source, and a double motorized rotation stage collected light as a function of the zenith angle with a resolution of 1°. Color measurement of CuO–PS CPhC films was calculated by SpectraSuite software (Ocean Optics) according to the Commission International d'Eclairage (CIE) standard colorimetric system. Raman spectra were analyzed from a reference database of KnowItAll Information System (Bio–Rad Laboratories).

Results and discussion

Optical properties of the CuO NPs

Cu is the most common used metal in electronics applications, because it is with conductivity and low cost. In this study, Cu is prone to surface oxidation that can significantly affect the optical properties. Therefore, we firstly

discussed the optical characteristics of the CuO NPs. Figure 2(a) shown the diluted solution appears black-brown because light is absorbed across the entire visible spectrum. Figure 2(c) illustrates the transmittance spectra of CuO NPs with different concentration, where the sample absorbs strongly in the visible spectrum, the transmittance drops to around 6% or less that depends on the concentration of CuO NPs. Figure 2(d) shown the measured extinction spectra, that depends on the size, shape, and aggregation state of CuO NPs[31], which is almost entirely photon absorption. Figure 2 demonstrates that surface adsorption CuO NPs on PS nanospheres could absorb visible light. Moreover, Fig. 2 shows that the absorbance degree of light, which is crucial for absorbing background and scattering light in CPhC color structures, was dependent on the CuO NPs content. In addition, scattering from a sample is typically very sensitive to the aggregation state of the sample, with the scattering contribution increasing as the particles aggregate to a greater extent[17]. When particles aggregate and the conduction electrons near each particle surface become delocalized and are shared amongst neighbouring particles. The extinction spectra of Figs. 2(b) and 2(d) were clearly demonstrated that the CuO NPs are agglomerating that caused the localized surface plasmon resonance of CuO NPs was not observed[17,30].

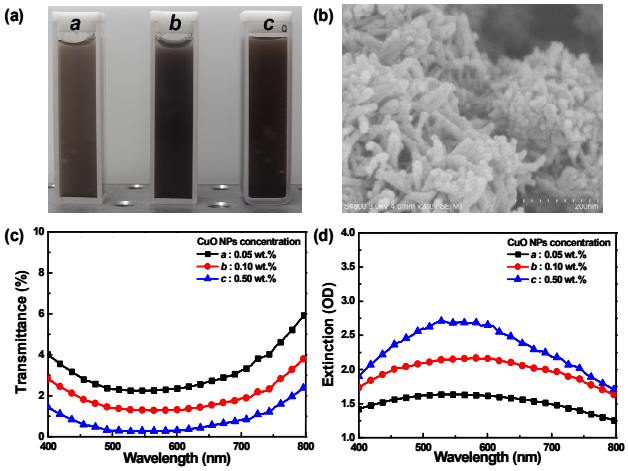

Figure 2. (a) The diluted solution appears black-brown due to the light is absorbed across the entire visible spectrum. (b) FESEM image of agglomerates of CuO NPs with 0.5 wt.% concentration. (c) Transmittance and (d) extinction spectra of CuO NPs solutions is almost entirely to light absorption with negligible scattering.

Crystal structures of the prepared CuO–PS CPhC color films

This work studied samples prepared with varying PS nanosphere sizes and different CuO NPs concentrations (Tab. S2). The CuO–PS CPhC color films were fabricated by the CuO NPs mixing of gravitational sedimentation method, as shown in Fig. 3(a). The gravitational sedimentation method enabled PS nanospheres to assemble into a highly crystalline arrangement with face-centered cubic (*fcc*) crystals[33]. CuO–PS mixture suspensions were dropped on the cover glass substrate and placed in an oven at a constant temperature of 50 °C for 2 h. The oven temperature was then raised to 80 °C for 30 min, and the treatment enhanced the physical rigidity of the CuO–PS CPhC color films. Figure 3(b) shows the photographs of PS CPhCs without and with CuO NPs. Pure PS CPhC films are usually milky white with extremely faint structural colors. As shown in Fig. 3(b), by introducing CuO NPs into PS CPhC structures, the visual appearance of PS CPhCs markedly changed from green to intense yellow. These pictures were obtained under normal natural lighting conditions and showed the highly orientation-dependent Bragg diffraction. These pictures provide a new color mechanism, which should contribute to the absorbance of light scattered by embedded CuO NPs. The key result in this study was obtained by introducing only 0.50 wt.% of CuO NPs into the CPhC structures, and the visual appearance of CPhC color films changed markedly (Fig. 3(b)). Detailed measurements of the angle optical spectra below strongly indicated that this effect was due to backward scattering absorption inside CPhC structures.

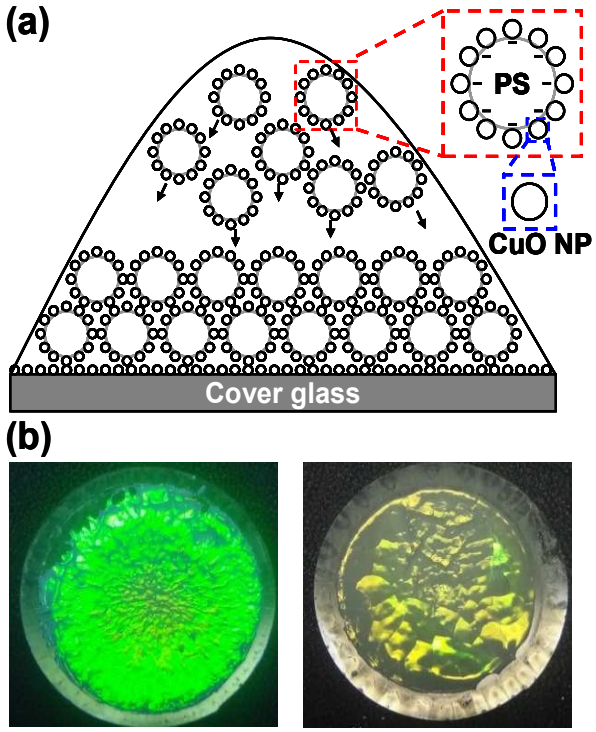

Figure 3. (a) Schematic showing the preparation of CuO–PS CPhC films using the gravitational sedimentation method. (b) Photographs of PS CPhC films prepared without (left) and with (right) CuO NPs.

We prepared three diameters of PS nanospheres, with D_{PS} of 190, 230, and 265 nm (Tab. S2). FESEM was used to study the crystalline structure of the CuO–PS CPhC films. The CuO–PS CPhC films with *fcc* structures were grown through gravitational sedimentation, with surfaces parallel to the (111) crystallographic plane. Figure 4(a) shows the uniformly sized nanospheres consisting of an *fcc* array. The FESEM images indicated that the CuO NPs dopant did not disrupt the

structures of CPhCs. The EDS mapping images of the CuO–PS CPhC films showed the CuO NPs random adsorbed on PS nanospheres (Fig. 4(b)). Figure 4(b) shows the EDS mapping images of a sample compared with Cu atoms and O atoms appear more often at the nanospheres; this indicates that surface oxidization occurred. In addition, the CuO–PS CPhC color film structures were also investigated by obtaining the Raman spectra, as shown in Fig. 4(c). In addition, the PS CPhCs and CuO structures were also measured by Raman spectra[34,35], respectively, as shown in Fig. S2. All Raman spectra were analyzed using a commercial library search (KnowItAll Information System) and literature[34,35]. We confirmed that the introduction of CuO NPs doping at these low concentrations did not affect the structural quality of the PS CPhC films.

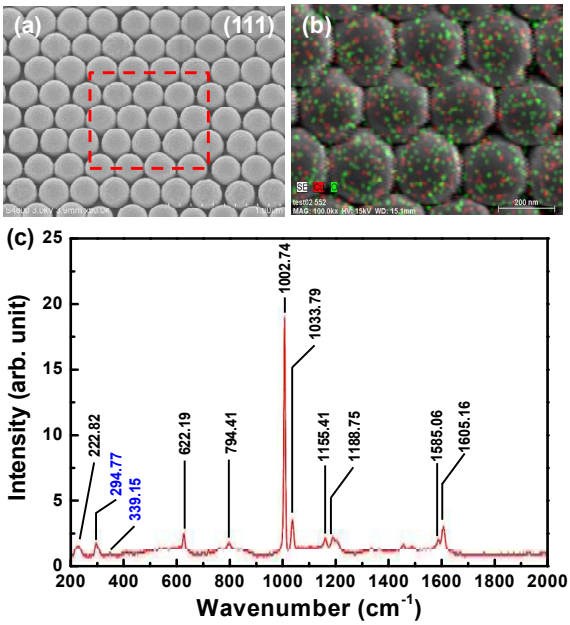

Figure 4. (a) SEM image of PS CPhC structures with 0.50 wt.% CuO NPs (sample C). (b) EDS compositional mapping (Cu/O overlay) scans from the red dashed line area of the image (a). (c) Raman spectrum of CuO–PS CPhC color films, in which black and blue indicate PS and CuO signals, respectively.

Effects of CuO NPs content on PS CPhC color films

Figure S1 shows that the CuO NPs were stably dispersed in the PS latex. The normal reflectance spectra of all samples were measured by a UV–Visible spectrometer with a Xe lamp. Figures 5, S3, and S4 revealed the reflectance spectra and photographs of PS CPhC films with and without CuO NPs, in which PS nanospheres were 230 (sample B), 190 (sample A), and 265 nm (sample C) in diameter, respectively. PS CPhC films without CuO NPs showed reflectance peaks at 452 (sample A), 547 (sample B), and 630 (sample C) nm, which corresponded to blue, green, and red, respectively. After doping 0.50 wt.% of CuO NPs to the three kinds of PS nanospheres, the color films displayed a low reflection intensity and broadband reflectance peaks at 459, 557, and 638 nm, which corresponded to cyan blue, yellow, and deep red, respectively. The reflectance spectra of PS CPhCs with various amounts of CuO NPs showed different reflection peak positions, which were in accordance with the Bragg law.

In addition, PS CPhC films containing 0.05 wt.% CuO NPs were observed to exhibit strong reflectance because of CuO NP content effect (Fig. 5(c)). With the increase in CuO NP content, the structural color became brilliant, because scattering and background light were strongly absorbed by settling on the bottom of CuO NPs (Fig. 5(b)). Conversely, excessive CuO NPs resulted in declined peak height and the loss brightness, because certain CuO NPs may cover the surfaces of PS nanospheres by hydrogen bonding or other molecular forces during self-assembly of PS nanospheres into the ordered structures[17,19-20], as shown in Figs. 5, S3, and S4. Thus, more photons were absorbed in the PSB. The brilliance of CPhC color films was effectively enhanced by adding an appropriate amount of CuO NPs. Bright structural colors (Fig. S3) were achieved because of the well-ordered structure, and film color was tunable by changing the size of PS nanospheres. The effects of the CuO NP content on the reflectance and color of CPhC films are summarized in Figs. 5 and S3, respectively.

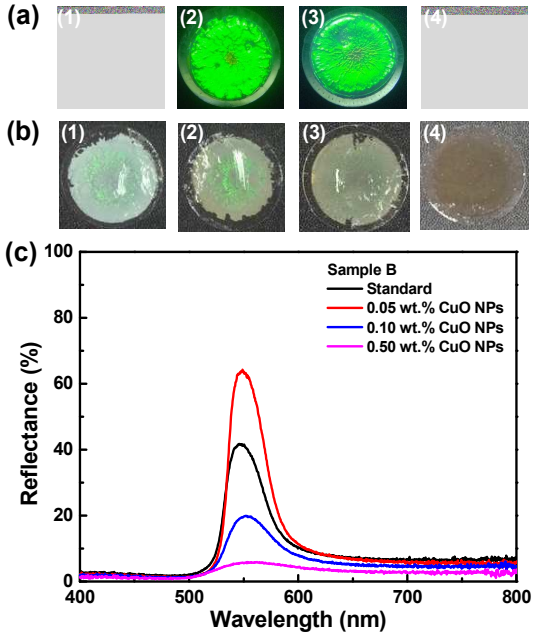

Figure 5. Top photographs show (a) the top surface and (b) the back surface of CuO–PS CPhC films (1) without CuO NPs (standard), (2) with 0.05, (3) with 0.10, and (4) with 0.50 wt.% CuO NPs, respectively. (c) Reflectance of PS CPhC films (sample B) without and with CuO NPs.

Angle–resolved specular reflection spectra were measured to study the PSB of the CuO–PS CPhC color films[14-15,31]. The angle-resolved specular reflection spectra, as a function of detection angle α, were obtained using a fiber probe coupled to an optical spectrometer. The optical spectrometer was rotated from 10° to 50° in increments of 1.0°, and the fiber-to-device distance was maintained at 15 cm. As Fig. 6 shows, when the incident angle α increased from 10° to 50°, the intensity of specular reflection decreased, accompanied with a

blue shift in the reflection peak. This phenomenon was the PSB of CPhC structures, suggesting that reflected light was dominated by the constructive interference of the reflected light. The theoretical wavelengths of Bragg diffraction of CuO–PS CPhCs were determined using the combined form of Bragg law and Snell law. For example, according to the Bragg–Snell law (Eq. (1)), the relationship between the reflection peak wavelength λ_R and incident angle α of an ordered structure is

$$\lambda_R = \sqrt{8/3} D_{PS} \sqrt{n_{eff}^2 - \sin^2 \alpha} \qquad (1)$$

where D_{PS} = 230 nm is the diameter of PS nanospheres (sample B with 0.50 wt.% CuO NPs) and λ_R = 557 nm at normal incident (α = 0°), respectively. We obtained the n_{eff} = 1.483 that is the effective refractive index of the medium. In this case, n_{CuO_air} was obtained using Eq. (2):

$$n_{eff} = \left[n_{PS}^2 f_{PS} + n_{CuO\_air}^2 \left(1 - f_{PS}\right) \right]^{1/2} \qquad (2)$$

where n_{PS} = 1.592[36] is the refractive indices of PS nanospheres, and f_{PS} = 0.74 is the volume fraction of the PS nanosphere, respectively. Therefore, we calculated to obtain n_{CuO_air} = 1.116 that is the refractive indices of CuO NPs. The reflection position slightly red shifted compared with the original PS CPhCs when CuO NPs had adsorbed on PS nanospheres. This adsorption was monitored based on the higher n_{CuO_air} than n_{air}, as shown in Fig. 4(b). In addition, the reflection measurement results showed that the PSB shifted toward shorter wavelengths as the detection angles increased. This trend indicated that light wave propagation was impossible within this region. The measured results were consistent with Fig. 5.

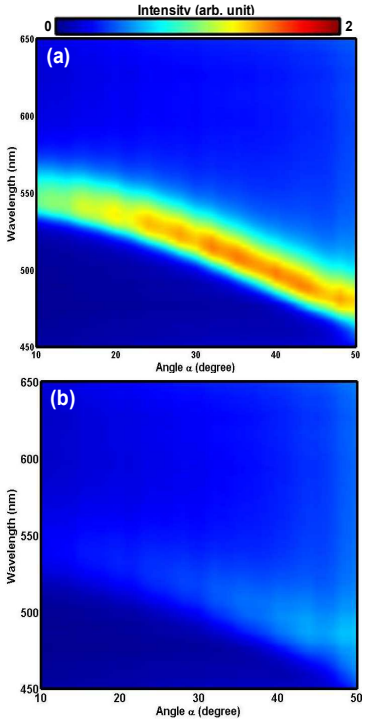

Figure 6. Angle–resolved specular reflection measurement of PS CPhC color films (sample B) (a) without and (b) with 0.50 wt.% CuO NPs.

Tunable structural colors of the CuO–PS CPhC color films

The color of CuO–PS CPhC films was determined by the corresponding chromaticity coordinates of the CIE standard colorimetric system. The visible wavelength (380 to 700 nm) of CIE chromaticity diagram visually determined the changes in CPhC structural colors. The color measurement of CuO–PS CPhC films was irradiated on a D65 light source of the CIE standard illuminant. Subsequently, the reflection spectra obtained from CuO–PS CPhC films were used to calculate CIE chromaticity coordinates according to SpectraSuite software. The color of CPhC structures was visually presented in the CIE chromaticity diagram, in which the color coordinates pointed to the corresponding structural color. For the PS nanospheres with diameters of 190 (sample A, ■), 230 (sample B, ●), and 265 (sample C, ▲) nm, Fig. 7 shows that the corresponding structural colors were blue, green, and red, respectively. With the same diameters of PS nanospheres, the incorporation of different CuO NPs corresponded to the same color hue but different color purities. Not only were the three primary colors for additive or subtractive combination achieved using the CuO–PS CPhCs, but iridescent derivative colors were also achieved by altering the diameters of PS nanospheres (Fig. 7). In addition, Fig. 7 exhibited the larger color shift of sample A (■) and sample B (●) than sample C (▲), because the reflection peak of sample C was much closed to cutoff wavelength (700 nm) of CIE chromaticity diagram. The CuO–PS CPhC color films exhibited considerable potentials to show not only panchromatic colors but also holographic colors. PS nanosphere size and CuO NP content could influence optical properties of CPhC color films.

Finally, all samples were stored at a room temperature and general relative humidity (RH) of 25 °C and 60 RH through three months. We have again measured the reflectance and the CIE chromaticity coordinates that results exhibited the long term stability, respectively, as shown in Figs. S5 and S6. Therefore, the practical CuO–PS CPhC color films did not suffer adverse effects according to the experimental results.

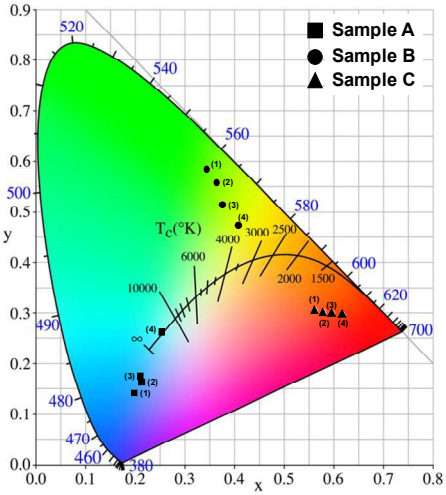

Figure 7. CIE chromaticity diagram of CuO–PS CPhC films with different sample (A–C) and CuO NPs contents.

Conclusions

In this study, CuO NPs doped into PS CPhC structures could absorb all wavelengths, remarkably increasing color and producing brilliant tunable structural colors that were visible under natural lighting conditions. Considering that the backward scattering of light was absorbed by embedded CuO NPs, the visual appearance of colloidal crystal coatings changed markedly from faint milky white to brilliant colors. In addition, the CuO–PS CPhC films were measured and predicted on the basis of with UV–Visible spectroscopy, FESEM, and EDS. This novel method offers tunable structural color for future applications in textile fabrics, bionic colors, and optical devices.

Acknowledgements

This work is supported by the Ministry of Science and Technology (MOST) in Taiwan, under contract numbers MOST102-2632-E-035-001-MY3, MOST103-2221-E-035-029, and MOST103-2622-E-035-007-CC2. The authors appreciate the Preci-sion Instrument Support Center of Feng Chia University in providing the fabrication and measurement facilities.

Notes and references

1 M. Srinivasarao, *Chem. Rev.*, 1999, **99**, 1935–1961.
2 P. Vukusic, and J. R. Sambles, *Nature*, 2003, **424**, 852–855.
3 R. A. Potyrailo, H. Ghiradella, A. Vertiatchikh, K. Dovidenko, J. R. Cournoyer, and E. Olson, *Nat. Photonics*, 2007, **1**, 123–128.
4 F. Marlow, Muldarisnur; P. Sharifi, R. Brinkmann, and C. Mendive, *Angew. Chem. Int. Ed.*, 2009, **48**, 6212–6233.
5 J. F. Forster, H. Noh, S. F. Liew, V. Saranathan, C. F. Schreck, L. Yang, J. G. Park, R. O. Prum, S. G. J. Mochrie, C. S. O'Hern, H. Cao, and E. R. Dufresne, *Adv. Mater.*, 2010, **22**, 2939–2944.
6 Y. Takeoka, *J. Mater. Chem.*, 2012, **22**, 23299–23309.
7 H. Noh, S. F. Liew, V. Saranathan, S. G. J. Mochrie, R. O. Prum, E. R. Dufresne, and H. Cao, *Adv. Mater.*, 2010, **22**, 2871-2880.
8 A. R. Parker, V. L. Welch, D. Driver, and N. Martini, *Nature*, 2003, **426**, 786–787.
9 H. Cong, B. Yu, and X. S. Zhao, *Opt. Express*, 2011, **19**, 12799–12808.
10 T. Zhang, Y. Ma, and L. Qi, *J. Mater. Chem. B*, 2012, **1**, 251–264.
11 A. Yethiraj, and A. V. Blaaderen, *Nature*, 2003, **421**, 513-517.
12 Y. Liu, J. Goebl, and Y. Yin, *Chem. Soc. Rev.*, 2013, **42**, 2610-2653.
13 S. Wong, V. Kitaev, and G. A. Ozin, *J. Am. Chem. Soc.*, 2003, **125**, 15589-15598.
14 C. F. Lai, C. L. Hsieh, and C. J. Wu, *Opt. Lett.*, 2013, **38**, 3612-3615.
15 C. F. Lai, Y. C. Lee, and C. T. Kuo, *J. Light. Technol.*, 2014, **32**, 1930-1935.
16 O. L. J. Pursiainen, J. J. Baumberg, H. Winkler, B. Viel, P. Spahn, and T. Ruhl, *Opt. Express*, 2007, **15**, 9553-9561.
17 C. I. Aguirre, E. Reguera, and A. Stein, *ACS Appl. Mater. Interfaces*, 2010, **2**, 3257–3262.
18 Y. Yamada, M. Ishii, T. Nakamura, and K. Yano, *Langmuir*, 2010, **26**, 10044–10049.
19 H. Cong, B. Yu, S. Wang, L. Qi, J. Wang, and Y. Ma, *Opt. Express*, 2013, **21**, 17831-17838.
20 W. Wang, B. Tang, W. Ma, J. Zhang, B. Ju, and S. Zhang, *J. Opt. Soc. Am. A*, 2015, **32**, 1109-1117.
21 D. Wang, V. S. Maceira, L. M. L. Marzan, and F. Caruso, *Adv. Mater.*, 2002, **14**, 908-912.
22 Z. Z. Gu, R. Horie, S. Kabo, Y. Yamada, A. Fujishima, and O. Sato, *Angew. Chem. Int. Ed.*, 2002, **41**, 1153-1156.
23 K. L. Kelly, E. Coronado, L. L. Zhao, and G. C. Schatz, *J. Phys. Chem. B*, 2003, **107**, 668-677.
24 S. L. Kuai, G. Bader, and P. V. Ashrit, *Appl. Phys. Lett.*, 2005, **86**, 221110-221113.
25 Y. Tan, W. Qian, S. Ding, and Y. Wang, *Chem. Mater.*, 2006, **18**, 3385-3389.
26 C. Noguez, *J. Phys. Chem. C*, 2007, **111**, 3806-3819.
27 M. O.A. Erola, A. Philip, T. Ahmed, A. Suvanto, and T. T. Pakkanen, *J. Solid. State Chem.*, 2015, **230**, 209-217.
28 J. P. Ruparelia, A. K. Chatterjee, S. P. Duttagupta, and S. Mukherji, *Acta Biomaterialia*, 2008, **4**, 707-716.
29 A. J. Vizcaino, A. Carrero, and J. A. Calles, *Int. J. Hydrogen Energy*, 2007, **32**, 1450-1461.
30 G. H. Chan, J. Zhao, E. M. Hicks, G. C. Schatz, and R. P. V. Duyne, *Nano Lett.*, 2007, **7**, 1947-1952.
31 C. F. Lai, C. C. Chang, M. J. Wang, and M. K. Wu, *Opt. Express*, 2013, 21, A687-A694.
32 S. J. Lee, S. H. Im, and K. J. Chae, *Macromol. Res.*, 2014, 22, 357-360.
33 G. Liu, L. Zhou, C. Wang, Y. Wu, Y. Li, Q. Fan, and J. Shao, *RSC Advances*, 2015, 5, 62855-62863.
34 M. Balkanski, M. A. Nusimovici, and J. Reydellet, *Solid State Comm.*, 1969, **7**, 815-818.
35 W. T, Yao, S. H. Yu, Y. Zhou, J. Jiang, Q. S. Wu, L. Zhang, and J. Jiang, *J. Phys. Chem. B*, 2005, **109**, 14011-14016.
36 S. N. Kasarova, N. G. Sultnova, C. D. Ivanov, and I. D. Nikolov, *Opt. Mater.*, 2007, **29**, 1481-1490.

Graphic for Table of Contens:

Preparation of Colloidal Photonic Crystal containing CuO Nanoparticles with Tunable Structural Colors

Chun-Feng Lai,* Yu-Chi Wang, Chia-Lung Wu, Jia-Yu Zeng, and Chia-Feng Lin

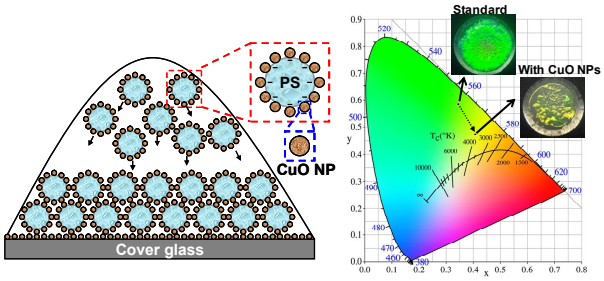

Polystyrene colloidal photonic crystal structures containing copper oxide nanoparticles present tunable structural colors, which are highly useful properties for applications.